Industrial-scale Manufacturing Experience of Titanium Beryllide Block for DEMO Blanket Application

Ramil Gaisin[a], Vladimir Chakin[a], Pavel Vladimirov[a], Francisco Alberto Hernandez Gonzalez[a], Sergey Udartsev[b], Anatoly Vechkutov[b], Maxim Kolmakov[b]

[a]*Karlsruhe Institute of Technology, Hermann-von-Helmholtz-Platz 1, 76344 Eggenstein-Leopoldshafen, Germany*
[b]*Ulba Metallurgical Plant, Abay Avenue 102, 070005 Ust-Kamenogorsk, Kazakhstan*

For the first time, the $TiBe_{12}$ blocks have been manufactured by powder metallurgy using industrial equipment at the Ulba Metallurgical Plant. Such blocks will be used for neutron multiplication in the helium-cooled breeding blanket for the EU DEMO fusion reactor. The vacuum annealing of a cold-pressed composite of Be and Ti powders at 600–1275°C approved the conditions for $TiBe_{12}$ synthesis. After hot isostatic pressing at 1150°C, a single-phase $TiBe_{12}$ structure was formed, but the sample fragmented into several pieces. These beryllide pieces were used to manufacture $TiBe_{12}$ powder. Vacuum hot pressing of the obtained powder resulted in a solid titanium beryllide workpieces of Ø150 mm × 170 mm. Electrical discharge machining and waterjet cutting were used to machine the external and internal surfaces in accordance with the design requirements.

The obtained block has a density of 98.3% of the theoretical density of $TiBe_{12}$. Microstructural analysis revealed a bimodal grain size distribution with grains of 5–10 μm and 20–40 μm. Electrical conductivity and thermal expansion coefficient of $TiBe_{12}$ are similar to other beryllides. To mimic the pulsed operating conditions in DEMO, a sample of titanium beryllide was rapidly heated to 900°C and cooled with a rate of 12 K/s. After 50 cycles, the sample had no cracks or severe surface oxidation.

Keywords: titanium beryllide; beryllide; synthesis; hot isostatic pressing; vacuum hot pressing; DEMO.

1. Introduction

Recently, hexagonal beryllide blocks have been proposed to be used as neutron multiplier in the helium-cooled breeding blanket (HCPB) for the DEMO fusion reactor [1]. Intermetallic titanium beryllide ($TiBe_{12}$) was chosen as a neutron multiplier material instead of pure Be, since $TiBe_{12}$ has an increased operating temperature, higher corrosion resistance, swells less and retains lower amount of tritium under irradiation [1-5]. Using beryllide removes the requirement of short diffusion path of tritium, which in former design was an additional motivitaion to use of beryllium in form of pebbles with a diameter of 1 mm. Instead of Be pebble bed, $TiBe_{12}$ can be used in the form of a hexagonal prismatic block of Ø144 mm × 150 mm with a 80 mm hole (Fig. 1) [1]. The key issue for the implementation of prismatic blocks in the HCPB breeding blanket design is to demonstrate feasibility of industrial production of large beryllide blocks in relevant amounts for the EU DEMO.

Various methods for the manufacture of relatively small titanium beryllide samples have been tested by many researchers in the past: casting [3, 6-7], rotating electrode method [3, 8-10], hot isostatic pressing [7, 11], vacuum hot pressing [12-14], and spark plasma sintering [15-16]. The current paper describes the first industrial-scale manufacture of full-sized $TiBe_{12}$ blocks obtained in cooperation between Karlsruhe Institute of Technology (KIT) and Ulba Metallurgical Plant (UMP) and their preliminary testing for thermal cycling stability.

2. Experimental

Beryllium (PTB-56, manufactured at UMP) and titanium (RP-Ti grade OM-1, JSC Polema) powders were chosen as the starting materials. Particle sizes of Be and Ti powders were <56 μm and <100 μm respectively. According to the certificate, Be PTB-56 powder consists of 98.93Be, 0.78O, 0.11Fe, 0.025Si, 0.019Mg, 0.019Al, 0.018Ni, 0.012Mn (wt.%). The maximum content of other elements is limited as follows (wt.%): 0.005Pb, 0.01Cu, 0.05C, 0.001F. A strong advantage of PTB-56 Be powder is its very low uranium content less than 0.4 ppm. Impurities in titanium powder are 0.35H, 0.2Fe, 0.2Ni, 0.1Si, 0.08N, 0.05C (wt.%). Beryllium powder particles are sharp-angled (Fig. 2a), whereas Ti powder particles often have irregular shapes (Fig. 2b).

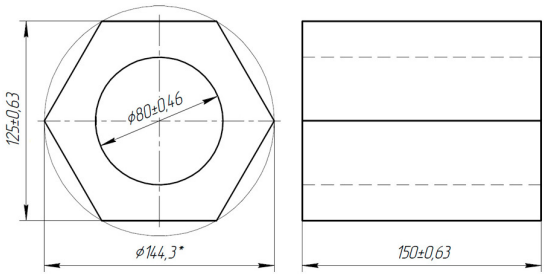

Fig. 1. Titanium beryllide block drawing in accordance with the enhanced helium-cooled breeding blanket design [1]

Be and Ti powders were blended together in a ratio of 70/30 respectively and were compacted to cylindrical composite samples of Ø30 mm × 50 mm using cold isostatic pressing (CIP). Be-Ti composite samples were annealed in vacuum in the temperature range of 650–1275°C for an hour. After annealing and cooling, the phase composition, dimensions and density were controlled.

ramil.gaisin@kit.edu

Hot isostatic pressing (HIP) was used to manufacture titanium beryllide powder. To do this, Be-Ti composites after CIP were sealed into steel capsules. After degassing, capsules were annealed at 1150°C for 5 hours in argon atmosphere with a pressure of 132 MPa. After dissolving the capsule shell in acids, the beryllide pieces were ground to powder.

At the last stage of sintering, vacuum hot pressing (VHP) was performed. VHP parameters are a trade secret of UMP and cannot be yet disclosed. After VHP, a hole with a diameter of 2 mm was drilled using a waterjet. In total, three workpieces of Ø150 mm × 170 mm were manufactured. The flat surfaces of the hexagon, as well as the internal hole of the required diameter and samples for investigations, were cut using an electrical discharge machining (EDM).

(a)

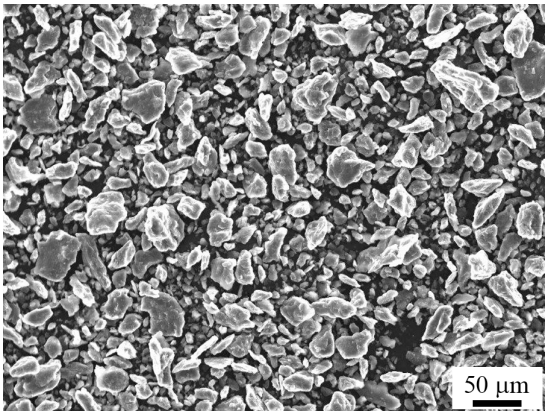

(b)

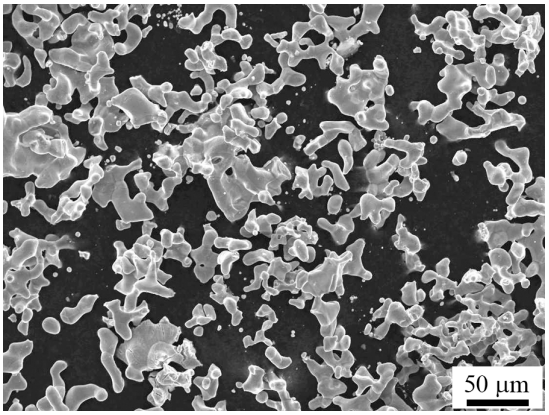

Fig. 2. Microstructure of powders: (a) Be, (b) Ti. SEM

The microstructure was studied using optical (OM) and scanning electron microscopy (SEM). X-ray diffraction (XRD) measurements were carried out using Cu-K$\alpha_{1/2}$ radiation in order to determine the phase composition. Microhardness was measured on PTM-3M tester using 200 gf indentation forces. Density was measured by the hydrostatic weighing method. In the paper, density is also presented as a percentage of theoretical density (TD). In the calculations, TD of $TiBe_{12}$ was 2.288 g/cm^3 [17], TD of Be-Ti composite (70/30) was 2.245 g/cm^3. Electrical conductivity was measured on Fischer Sigmascope SMP10 using the eddy current method. Netzsch DIL 402 was used for dilatometry at 300–1000°C temperature range.

A sample of $TiBe_{12}$ after VHP with a size of Ø19 mm × 21 mm was used for thermocycling experiment in air. The sample was inductively heated 200–900°C for 60 sec, annealed at 900°C for 45 sec, and cooled in a stream of compressed air to 200°C for 60 sec. The number of heating and cooling cycles was 50. A fragment of an induction furnace together with a heated sample is represented in Fig. 3.

Fig. 3. Induction heating of a $TiBe_{12}$ sample during thermocycling

3. Results

3.1 Vacuum annealing

The work began with experiments on the synthesis of $TiBe_{12}$, based both on the long-term experience on development of beryllium-based materials at KIT and on the know-how of tantalum beryllide manufacturing at UMP. The main conditions of titanium beryllide synthesis during HIP have been already determined in KIT [7]. UMP has successfully used CIP for the production of tantalum beryllide samples with Ø90 mm × 90 mm. Therefore, CIP has been selected for the initial compaction of pure beryllium and titanium powders.

After the CIP of Be and Ti powders, the density of the composite samples was measured as 1.45–1.60 g/cm^3. This corresponds to 65–71% of Be-Ti composite TD. In comparison with hot extrusion [7, 18], the obtained density is much lower, since Be and Ti powders were not supposed to deform so well at room temperature.

With the aim to study the synthesis conditions of $TiBe_{12}$, vacuum annealing experiments at 650–1275°C of Be-Ti composites after CIP were performed. After annealing, the phase composition of each sample was determined, and the density, diameter, and height of the samples were measured.

Fig. 4 represents XRD patterns of cold-pressed and annealed Be-Ti samples. The cold-pressed composite and the sample after annealing at 650°C are composed of only Be and Ti phases. Dimensions and density of the

sample after annealing at 650–700°C did not change (Fig. 5). After annealing at 800°C, peaks of the intermetallic $TiBe_{12}$ and $TiBe_2$ phases appeared on the XRD patterns and the intensity of Ti and Be peaks decreased (Fig. 4).

The diameter and height of the sample increased by about 10%, and the density decreased by 20% (Fig. 5). Annealing at 1100–1275°C resulted in the same diffraction patterns with a single phase $TiBe_{12}$ structure. Samples after annealing at these highest temperatures swelled up to 35–50% with a decrease in density up to 65%.

The observed swelling and decrease in density can be explained by the Kirkendall effect. The difference in diffusion rates of Be and Ti atoms in Ti and Be respectively result in porosity in the former places of Be. An increase in Be porosity was observed in the cast Be-Ti pebbles after annealing and in the hot-extruded Be-Ti composite after HIP [7, 9].

According to XRD measurements, $TiBe_{12}$ begins to synthesize between 650 and 800°C. However, the annealing time and temperature were insufficient to obtain a single-phase $TiBe_{12}$ structure compared to the annealing at 1100–1275°C. An increase in the temperature from 1100°C to 1275°C did not lead to significant changes in the phase composition, dimensions, or density. This means that the complete synthesis of $TiBe_{12}$ can occur within one hour of annealing already at a temperature above 1100°C, and a further increase in temperature is not reasonable. After beryllide synthesis, the density reduces to 60%, and the material can have very high porosity and poor mechanical properties. This is unacceptable for neutron multiplier material, since the tritium breeding ratio decreases, and tritium can be retained in pores and voids. To increase the density of titanium beryllide, synthesis can be carried out at high pressure, e.g. high pressure argon atmosphere during HIP. The synthesis temperature should be above 1100°C, and the annealing time is more than one hour to obtain a single-phase $TiBe_{12}$ microstructure.

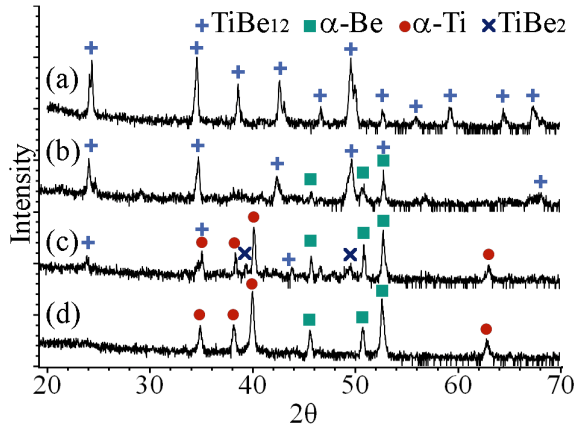

Fig. 4. X-ray diffraction patterns of compacted Be-Ti samples after annealing: (a) 1100–1275°C, (b) 1000°C, (c) 800°C, (d) 650°C

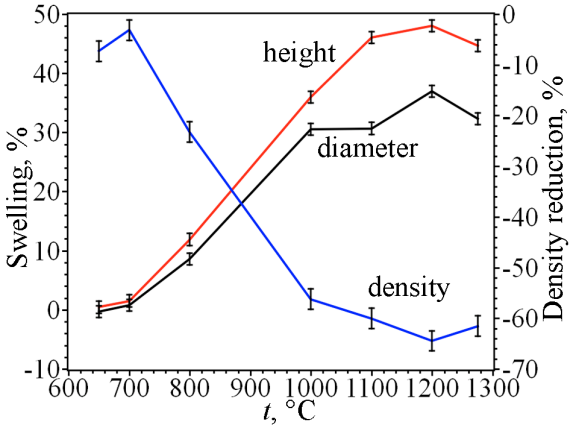

Fig. 5. Effect of annealing temperature on the height, diameter, and density of compacted Be-Ti samples

3.2 Hot isostatic pressing

In order to manufacture a titanium beryllide block of comparable size using HIP, a Be-Ti composite was compacted in the form of a cylinder with dimensions of Ø100 mm × 100 mm. After CIP, the composite was turned to the size of a steel capsule, and a hole was drilled in the center. A graphite cylinder with a diameter of 30 mm was inserted into this hole. Fig. 6 shows the composite sample with the graphite insert before sealing the capsule. The graphite insert was initially supposed to provide easy drilling after HIP. In the case of a titanium beryllide solid block, drilling is more difficult due to the very high hardness and brittleness of $TiBe_{12}$ [2, 7]. After sealing the capsule, it was degassed at a temperature of 650°C.

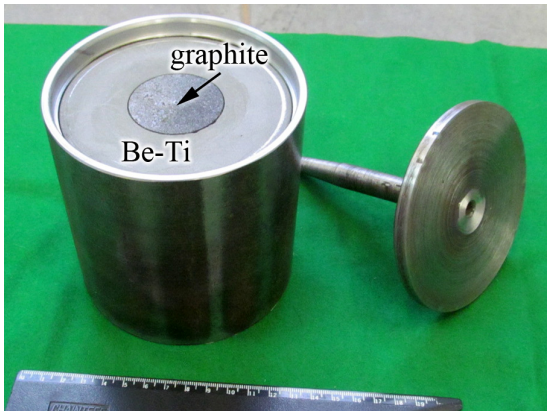

Fig. 6. Compacted Be-Ti sample with graphite insert in the steel capsule before HIP

After HIP at 1150°C, the capsule shell was removed and dissolved in etchant. Fig. 7 shows that the block fragmented into debris mainly in the radial direction. XRD (not presented) indicated that a single-phase $TiBe_{12}$ structure was formed during HIP. The density of $TiBe_{12}$ reaches 2.13 g/cm^3 or 93.1% of TD.

Fig. 7. $TiBe_{12}$ debris after HIP at 1150°C

It can be concluded that after HIP, a $TiBe_{12}$ structure was formed as well as after vacuum annealing at 1100–1200°C. However, high pressure at HIP led to an increase in density up to 93.1% of TD, whereas after vacuum annealing at 1100–1200°C, the density was only 25–28% of TD. The obtained density after HIP is still much lower compared to the titanium beryllide density in our previous work after HIP and hot extrusion (98.6% of TD [7]). The main reason for the lower density after HIP is the use of a less dense Be-Ti composite after CIP. The reasons of $TiBe_{12}$ fracture during HIP were not studied in details. The ductility of porous $TiBe_{12}$ after HIP seems to be not sufficient to relax thermal stress during HIP and heating/cooling of the capsule.

To find out whether the presence of the graphite insert caused the fracture of the block, one more HIP of the solid Be-Ti composite without an internal hole was carried out. However, without a graphite insert and with slower heating and cooling rates of the capsule, the block was fractured as well. Thus, HIP after CIP resulted in $TiBe_{12}$ debris, which could not be used as a neutron multiplier, but can be used for the manufacture of $TiBe_{12}$ powder. Therefore, HIP was used as an intermediate step for $TiBe_{12}$ synthesis to obtain its powder.

3.3 Vacuum hot pressing

Generally, HIP and VHP are the main methods of manufacturing parts from beryllium powder [12]. In the case of titanium beryllide, the HIP of a bigger Be-Ti samples led to cracking. Therefore, it was logical to switch to VHP for the manufacture of a titanium beryllide block.

Fig. 8 represents the microstructure of the $TiBe_{12}$ powder prepared from debris after HIP. The powder consists of irregular in shape particles of 10–100 µm. The powder was compacted to the cylindrical sample of Ø50 mm × 50 mm using CIP. The sample was placed in a graphite mold. After VHP processing, the block did not crack and generally retained its shape, only the corners of the block were slightly chipped when the sample was removed from the mold (Fig. 9). The density after VHP was 2.26 g/cm^3 or 98.8% of TD.

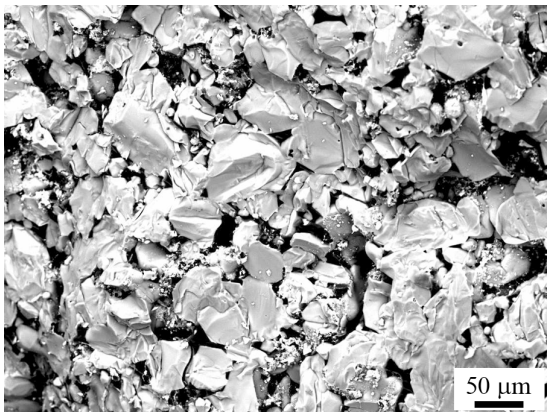

Fig. 8. Microstructure of $TiBe_{12}$ powder used for vacuum hot pressing

Since beryllides are very hard and brittle materials [12], EDM was used to cut flat surfaces and the inner hole. To cut the inner surface, initially a hole with a diameter of 2 mm was drilled using a waterjet. Fig. 10 shows a reduced in size block mockup with Ø41 mm × 22 mm after VHP and machining. No cracks were observed on the surface of the mockup.

Fig. 9. $TiBe_{12}$ sample after vacuum hot pressing

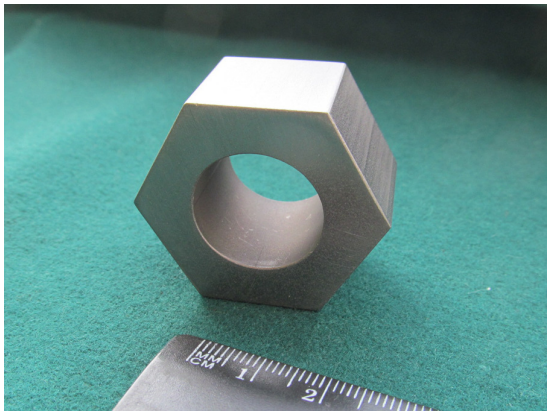

Fig. 10. $TiBe_{12}$ reduced in size mockup of the hexagonal block

A sufficient amount of titanium beryllide powder was prepared by HIP to manufacture three full-sized blocks. Three $TiBe_{12}$ compacted workpieces were subjected to VHP in graphite molds under the same conditions as a small workpiece. After VHP, workpieces of Ø150 mm × 170 mm were obtained (Fig. 11). The

workpieces had no surface cracks, only chips of 2–5 mm along sharp edges are observed. The density was 2.25 g/cm^3 or 98.3% of TD. The hole in the center and the flat surfaces of the full-sized block were cut using waterjet and EDM. Fig. 12 depicts the block after final machining. The block has no visible cracks or porosity on the surface.

Fig. 11. $TiBe_{12}$ full-sized workpiece after vacuum hot pressing

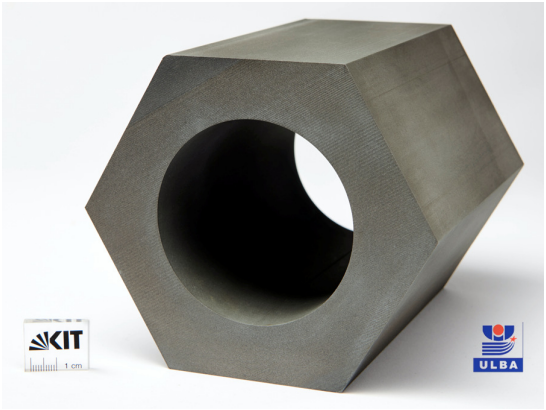

Fig. 12. Hexagonal $TiBe_{12}$ block after final machining

The structure and properties of the material after VHP were investigated on the material rests remained after cutting the flat surfaces and holes of the blocks and mockup. On XRD spectrum (Fig. 13), only peaks of $TiBe_{12}$ phase were detected. Fig. 14 shows SEM and OM microstructure of beryllide sample after VHP. It consists of a bimodal microstructure with fine grains of 5–10 µm and large grains of 20–40 µm. Large grains sometimes have contrasting boundaries inside. Some triple joints have pores. The porosity measured in four OM pictures averaged to 1.9%. The structure has no visible cracks. Microhardness measurements showed that intermetallic $TiBe_{12}$ after VHP has a hardness of 1000–1030 HV.

After VHP, $TiBe_{12}$ has a bimodal grain size distribution that is often observed in powder materials such as ODS-steels [19-21]. The reason for the rapid growth of some grains of $TiBe_{12}$ remains unknown. Generally, VHP resulted in a larger grain size of 5–40 µm compared to HIP with 0.3–2.5 µm [7]. This may cause lower hardness after VHP compared to HIP. On the other hand, a larger grain size and lower hardness can increase fracture toughness, which is important because the neutron multiplier is to operate under rapid heating and cooling conditions. A detailed study of the microstructure and mechanical properties is to be performed.

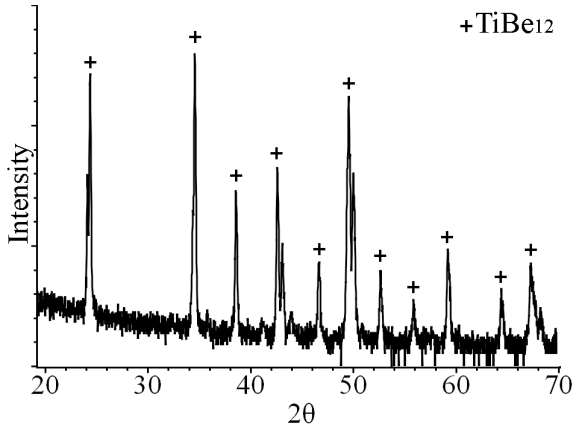

Fig. 13. X-ray diffraction pattern of a sample after vacuum hot pressing

(a)

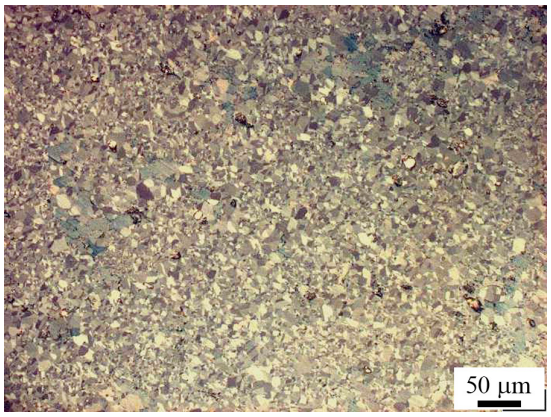

(b)

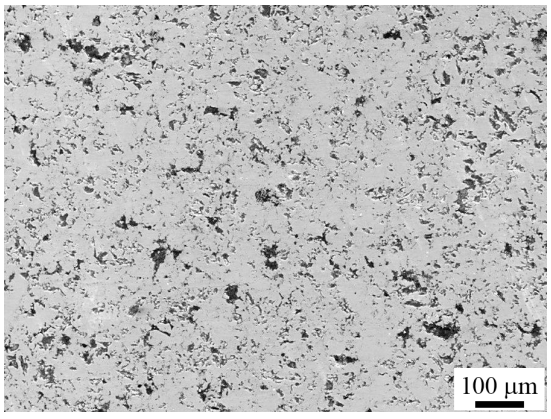

Fig. 14. Microstructure of $TiBe_{12}$ after vacuum hot pressing: (a) OM in polarized light, (b) SEM

In accordance with the pulsed operation of DEMO, the neutron multiplier blocks of $TiBe_{12}$ will experience relatively fast heating and cooling rates over several thousand cycles. To mimic such operating conditions, a preliminary experiment on accelerated thermocycling has been carried out. Fig. 15 shows the thermo-kinetic diagram of the thermal cycling. Fig. 16 represents $TiBe_{12}$ sample after thermocycling and the microstructure of its surface. Neither cracks nor severe oxidation were observed after 50 cycles of heating/cooling. The surface of the sample remained shiny.

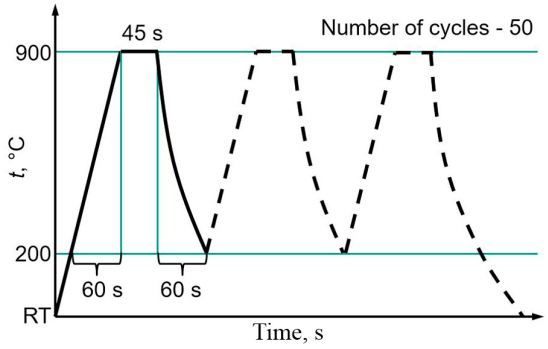

Fig. 15. Thermokinetic diagram of the performed thermocycling

(a)

(b)

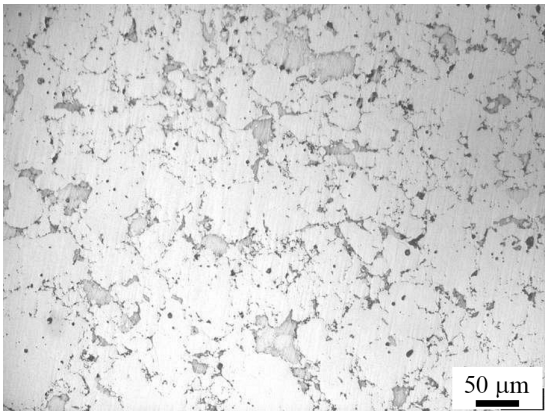

Fig. 16. (a) $TiBe_{12}$ sample after thermocycling, (b) OM of the surface of the same sample

At the next stage, the structure and properties of the obtained titanium beryllide after VHP will be studied in details. A full-scale thermal cycling experiment will be performed on a beryllide block manufactured in the work.

5. Conclusions

For the first time, hexagonal $TiBe_{12}$ block of Ø144 mm × 150 mm was manufactured. The manufacturing method is based on vacuum hot pressing of $TiBe_{12}$ powder. In total, three workpieces of titanium beryllide with Ø150 mm × 170 mm were manufactured. The powder was obtained from $TiBe_{12}$, synthesized by hot isostatic pressing at the first stage.

Experiments on vacuum annealing of cold-pressed Be-Ti composites showed that complete synthesis of titanium beryllide can occur during annealing at temperatures above 1100°C for 1 hour. Hot isostatic pressing at 1150°C and high argon pressure led to a single-phase $TiBe_{12}$ structure, but the sample always cracked and fractured during the processing.

The final product has a bimodal microstructure with fine grains of 5–10 µm and large grains of 20–40 µm. The microhardness was measured as 1000–1030 HV. $TiBe_{12}$ has electrical conductivity of $5.1 \cdot 10^6$ S/m and a coefficient of thermal expansion of $7.6–8.8 \cdot 10^{-6}$ K^{-1}. The titanium beryllide sample did not fracture or crack after 50 cycles of thermocycling with heating up to 900°C.

Acknowledgments

This work has been carried out within the framework of the EUROfusion Consortium and has received funding from the Euratom research and training programme 2014–2018 and 2019–2020 under grant agreement No 633053. The views and opinions expressed herein do not necessarily reflect those of the European Commission.

References

[1] F.A. Hernández, P. Pereslavtsev, G. Zhou, B. Kiss, Q. Kang, H. Neuberger, V. Chakin, R. Gaisin, P. Vladimirov, L.V. Boccaccini, G.A. Spagnuolo, S. D'Amico, I. Moscato, Advancements in the Helium-Cooled Pebble Bed Breeding Blanket for the EU DEMO: Holistic Design Approach and Lessons Learned, Fusion Science and Technology 75 (2019) 352–364.

[2] H. Kawamura, E. Ishitsuka, K. Tsuchiya, M. Nakamichi, M. Uchida, H. Yamada, K. Nakamura, H. Ito, T. Nakazawa, H. Takahashi, S. Tanaka, N. Yoshida, S. Kato, Y. Ito, Development of advanced blanket materials for a solid breeder blanket of a fusion reactor, Nuclear Fusion 43 (2003) 675–680.

[3] J.-H. Kim, M. Nakamichi, Comparative study on arc-melted and plasma-sintered beryllides, Journal of Alloys and Compounds 546 (2013) 171–175.

[4] J. Shimwell, L. Lu, Y. Qiu, P. Pereslavtsev, A. Häußler, F. Hernández, C. Zeile, T. Eade, G.A Spagnuolo, S. McIntosh, L. Packer, T. Barrett, Automated parametric neutronics analysis of the Helium Cooled Pebble Bed breeder blanket with $Be_{12}Ti$, Fusion Engineering and

Design 124 (2017) 940–943.
[5] Y. Mishima, N. Yoshida, H. Kawamura, K. Ishida, Y. Hatano, T. Shibayama, K. Munakata, Y. Sato, M. Uchida, K. Tsuchiya, S. Tanaka, Recent results on beryllium and beryllides in Japan, Journal of Nuclear Materials 367-370 (2007) 1382–1386.
[6] M. Uchida, H. Kawamura, M. Uda, Y. Ito, Elementary development for beryllide pebble fabrication by rotating electrode method, Fusion Engineering and Design 69 (2003) 491–498.
[7] R. Gaisin, V. Chakin, R. Rolli, J. Hoffmann, H. Leiste, T. Bergfeldt, U. Jäntsch, M. Klimenkov, J. Lorenz, A. Goraieb, P. Vladimirov, A. Möslang, Synthesis of $Be_{12}Ti$ compound via arc melting or hot isostatic pressing, Journal of Alloys and Compounds 818 (2020) 152919.
[8] P.P. Liu, L.W. Xue, W. Hu, L.P. Yu, H.F. Zhao, K. Wang, F.J. Xue, Y.M. Jia, Q. Zhan, F.R. Wan, Mechanical compression behaviors of single phase Be and binary $Be_{12}Ti$ pebbles, Fusion Engineering and Design 144 (2019) 202–208.
[9] V. Chakin, R. Rolli, R. Gaisin, P. Kurinskiy, J.-H. Kim, M. Nakamichi, Effect of heat treatment of titanium beryllide on tritium/hydrogen release, Fusion Engineering and Design 137 (2018) 165–171.
[10] J.-H. Kim, M. Nakamichi, Optimization of synthesis conditions for plasma-sintered beryllium–titanium intermetallic compounds, Journal of Alloys and Compounds 577 (2013) 90–96.
[11] P. Kurinskiy, V. Chakin, A. Moeslang, R. Rolli, A.A. Goraieb, H. Harsch, E. Alves, N. Franco, Characterisation of titanium beryllides with different microstructure, Fusion Engineering and Design 84 (2009) 1136–1139.
[12] K.A. Walsh, Beryllium Chemistry and Processing, ASM International, 2009.
[13] L.A. Jacobson, R.J. Hanrahan Jr., J.L. Smith, Beryllides, in: Intermetallic Compounds - Principles and Practice, John Wiley & Sons, Ltd, 2002, pp. 37–51.
[14] C.K. Dorn, W.J. Haws, E.E. Vidal, A review of physical and mechanical properties of titanium beryllides with specific modern application of $TiBe_{12}$, Fusion Engineering and Design 84 (2009) 319–322.
[15] J.-H. Kim, M. Nakamichi, Optimization of synthesis conditions for plasma-sintered beryllium–titanium intermetallic compounds, Journal of Alloys and Compounds 577 (2013) 90–96.
[16] J.-H. Kim, M. Miyamoto, Y. Hujii, M. Nakamichi, Reactivity and deuterium retention properties of titanium-beryllium intermetallic compounds, Intermetallics 82 (2017) 20–25.
[17] G.V. Samsonov and I.M. Vinitskii, Handbook of Refractory Compounds (translated from the Russian by Kenneth Shaw). IFI/Plenum Press, New York, 1980.
[18] P. Kurinskiy, H. Leiste, A. Goraieb, R. Rolli, S. Mueller, J. Reimann, A. Moeslang, Production of Be-Ti and Be-Zr rods by extrusion and their characterization, Fusion Engineering and Design 136 (2018) 49–52.
[19] T. Gräning, M. Rieth, J. Hoffmann, A. Möslang, Production, microstructure and mechanical properties of two different austenitic ODS steels, Journal of Nuclear Materials 487 (2017) 348–361.
[20] J. Hoffmann, M. Rieth, L. Commin, S. Antusch, Microstructural anisotropy of ferritic ODS alloys after different production routes, Fusion Engineering and Design 98-99 (2015) 1986–1990.
[21] A. Chauhan, D. Litvinov, J. Aktaa, High temperature tensile properties and fracture characteristics of bimodal 12Cr-ODS steel, Journal of Nuclear Materials 468 (2016) 1–8.